Characterization of the Interface/ Interphase in Natural Fibre Based Composites

Nicolas Le Moigne (1) , Belkacem Otazaghine (1) , Stéphane Corn (1) , Helene Angellier-Coussy (2) , Anne Bergeret (1)

(1) C2MA, IMT Mines Alès, Alès, France
(2) UMR IATE - Ingénierie des Agro-polymères et Technologies Émergentes

There are currently no standardized methods to assess the quality of the interface/ interphase in natural fibre reinforced composites. Nevertheless different approaches have been developed and are widely used by the scientific and industrial communities. These include microscopic and physico-chemical analyzes as well as micromechanical tests on model microcomposites and macroscopic mechanical tests on composite specimens. This last chapter proposes a review of the experi-mental techniques modelling approaches used to investigate the interface/interphase in natural fibres composites and quantify the interfacial adhesion.

5.1 Microstructural Analysis of the Interphase

5.1.1 Microscopic Analysis

Scanning Electron Microscopy (SEM) has proved to be a key tool for investigating the microstructure of composites made of lignocellulosic fibres and polymer matrix. SEM analyses provide direct visualization of the morphology at the filler/matrix interface. The qualitative criteria are mainly the occurrence of failure surfaces, fibre pull-outs, interfacial gaps around the fibres and debonding, or wetting of fibres by the polymer (Fig. 5.1). As observed for example for wood fibre-reinforced polyurethane composites (Rials et al. 2001), strong interfacial adhesion between the two phases was deduced from the observation of failure surfaces with a distinct fibre fracture without pull-out which is characteristic of a cohesive interfacial failure. In contrast, mostly fibre pull-out would be observed in the case of an adhesive interfacial failure. SEM observations are generally performed on manually cryo-fractured surfaces, which can induce bias in the observation of the morphology of surface failures. Indeed, the material is violently cooled, which might generate gaps between fibres and matrix, due to differences of thermal shrinkage between both components (Berthet et al. 2015). As

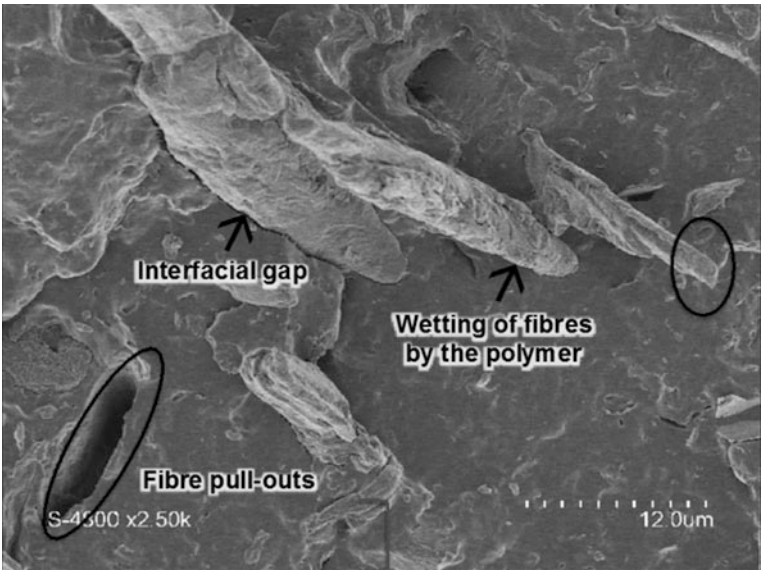

Fig. 5.1 SEM picture of cryo-fractured surface of PHBV/wheat straw fibres (20wt%) composites

performed by Bledzki and Jaszkiewick (2010), it sounds reasonable to only use SEM as a qualitative mean to compare the fibre/matrix interfacial adhesion in different formulations and to discriminate different failure surface morphologies. As compared to "classical" SEM analysis, the advantage of environmental scanning electron microscopy (ESEM) is the possibility to characterize wet, oily or electrically non-conductive samples without preliminary preparation and operating at relatively high pressures (George et al. 2001; Wright and Mathias 1993; Singh et al. 2013).

In situ observations of crack propagation by ESEM (equipped with an in situ tensile apparatus) could be useful to monitor failure mechanisms at the interface of biocomposites (see also Chap. 5, Sect. 2.1) and thus, provide qualitative information on the quality of the fibre/matrix interface. As showed for polylactic acid (PLA)/flax fibres composites (Le Moigne et al. 2014), this technique allows discriminating adhesive interfacial failure (due to the decohesion of the fibres and characterized by a clean break of the matrix) from cohesive interfacial failure (characterized by the tearing of the matrix and the breaking of the fibres). When ESEM is combined with X-ray energy analysis, the elemental composition of the surface can be determined using energy dispersive analysis of X-rays (EDX). The principle of ESEM-EDX consists in bombarding a specimen with an electron beam of sufficient energy with the emission of X-rays characteristics of each element present. Based on its specific energy and intensity, the atomic number and relative concentration of a particular element can then be determined. For example, Wright and Mathias (1993) used EDX to evidence that poly(EHMA) (homopolymer of ethyl alpha-hydroxymethylacrylate) and wood fibres were strongly bonded, through the presence of poly (EHMA) and its copolymers within the wood cell walls.

Polarized Optical Microscopy (POM) and transcrystallization. In the case of semi-crystalline polymers, POM observations of the crystallization phenomenon from the melt can be used to highlight the occurrence (or not) of interfacial transcrystallization and/or particle nucleating effect, both indicators of filler/matrix interactions (Wurm et al. 2010). Transcrystallization may reduce the final crystallinity degree of the matrix due to the reduced mobility of polymer chains as a consequence of the fast formation of high density nuclei on the filler surface (Luduena et al. 2012). As reported by Luduena et al. (2012), several parameters affect this process: the nature of the fibre, their surface roughness and surface treatment, the thermal conductivity of the fibre, and the processing conditions of composites.

As showed by Wang et al. (2011) for sisal/PLA systems, sisal fibres un-treated or treated with alkali or aminosilane (APS) have a nucleating ability and induce transcrystallinity in PLA matrix. When placed under isothermal crystallization conditions between 123 and 130 °C, first nuclei appeared preferentially at the fibres surface. Based on the theory of heterogeneous nucleation, the authors found that interfacial free energy difference functions of PLA for untreated and treated fibres were similar, suggesting that fibre surface modifications by using alkali or APS silane has no significant influence on the nucleation ability of sisal fibres in PLA matrix. Based on these results, the authors assumed that, although being influenced by fibre treatments, the surface energy of the fibre is not a critical factor for the development of transcrystallinity. They also pointed out that surface topography rather than surface chemistry might induce the nucleation process. Indeed, treated and untreated sisal fibres all had rough surfaces, providing abundant nucleation sites to induce transcrystallinity in PLA.

Joseph et al. (2003) also found that the surfaces of sisal fibre act as nucleating sites for the crystallisation of PP, promoting the growth of spherulites perpendicular to the fibres surface and forming a transcrystalline region around the fibre. Depending on the crystallization conditions (temperature, time and stress), the thickness of the transcrystalline layer varied from about 5 μm to more than 11 μm. The authors found that longer crystallization time and higher crystallization temperature, as well as stress induced crystallisation favour the formation of a thicker transcrystalline layer. As observed by Wang et al. (2011), fibre surface treatment with toluene-2, 4-diisocyanate (TDI)/polypropylene glycol (PPG) had limited effect on the nucleating ability of sisal fibres and transcrystallization of PP.

It is worth noting that POM samples are generally prepared between two glass slides, which constraints the material to crystallize with a limited mobility, possibility favouring the occurrence of cracks at the fibre/matrix interface and in the polymer phase during the crystallization process (Berthet et al. 2015).

Atomic force microscopy (AFM). Non-destructive methods such as AFM in tapping or force modulation modes could be used to characterize the physical properties (i.e. mainly the stiffness and visco-elastic behaviour) of composite interphases depending on the interaction forces between a sharp tip suspended on a very soft spring called cantilever and the sample surface, allowing to deduce interphase thickness (Mai et al. 1998). The lateral resolution of the AFM (related to the curvature radius of the probe) is typically of the order of 10 to 30 nm even if it is still possible to identify and

localize objects with dimensions down to the nanometre (e.g. carbon nanotubes). The depth resolution is of the order of the ångström. The sizes of analysed zones can vary from 1 μm × 1 μm to 100 μm × 100 μm. The development of scanning thermal microscopy (SThM), combined to AFM, allowed researchers to evaluate the thermal properties of materials (such as the glass transition temperature) at the microscopic scale (Tillman et al. 2000). AFM is also able to provide 3D images of topography, various interaction forces with molecular resolution within a thin layer of material and therefore gives an indication of the interfacial adhesive forces, as shown on wood-plastic composites (Effah et al. 2015). This is based on the knowledge of the depth of analysis, which is system dependent. AFM is not limited to topographic images; it can also be used to identify and discriminate surfaces that differ from their chemical properties by using modified AFM probes. In that case, called chemical force microscopy (CFM), the instrument detects the chemical interactions between the functionalized tip and the material surface. Among the constraints that have to be taken into account in the case of lignocellulosic fibre based composites, the surface roughness must be in the order of 100 nm or lower than the imaged zones, which imposes an adequate method of cutting and/or polishing of samples. The size of analysed particles must be compatible with the lateral resolution of the AFM (related to the radius of the probe), typically of the order of 10 nm. Finally, the respective hardness of the matrix and the particles will determine the maximal depth of analysis.

X-ray computed tomography. A visual analysis of the 3D structure, including the 3D porosity and distributed voids, can be done by X-ray computed tomography, as already done for glass fibre/polypropylene (Kastner et al. 2012) or carbon fibre/epoxy composites (Nikishkov et al. 2013; Yang and Elhajjar 2014). X-ray computed tomography is a non-destructive, powerful technique that provides a volumetric map of a specimen in three dimensions, generated from a series of X-ray projections of the samples recorded at different angles. It allows to quantitatively analyze the filler dispersion on macroscopic length scales. Continuous improvements in the quality and performance of X-ray tubes, detectors and devices have led to cone beam X-ray computed tomography systems, which can now achieve spatial resolutions down to 1 μm and even below, *i.e.* 50 nm in the case of nano-tomographs. Applications of high-resolution X-ray computed tomography are possible even when the density differences between the constituents are rather low, as recently reported for carbon fiber reinforced polymers (Kastner et al. 2012). By applying various 3D-filters, authors succeeded in extracting from the X-ray computed tomography data the following quantitative information and values: filler percentage, 3D-geometry of the fillers (diameter, surface, volume), fibre length distribution, filler orientation, 3D filler distribution, filler interconnectivity, porosity. In the case of biocomposite materials, the main limit will be the difference of density between the lignocellulosic fibres and the polymer matrix that may be too low to obtain exploitable images.

Alemdar et al. (2008) were among the first authors to use X-ray micro-tomography to study the effect of fibre separation techniques (enzyme treated and carded hemp fibres) and coupling agent (MAPP) on the microstructure and fibre size distribution in wood and hemp fibre reinforced PP composites. It was shown that the use of MAPP coupling agent in wood/PP composites resulted in a significant decrease of fibre

breakage during processing, and hence higher fibre length and width, possibly due to the lubricant effect of low molecular MAPP contributing to the shear stress reduction during processing. Smaller width distribution, higher aspect ratio and more uniform fibre distribution were observed for carded and enzyme treated hemp fibres/PP composites, highlighting the interest of these fibre separation techniques for composites applications. Some other interesting results were found by Martin et al. (2013) on PP/flax fibres biocomposites. X-ray micro-tomography observations of injection molded samples revealed greater fibre bundle splitting for higher retting degree of flax fibres. The authors also found a relatively low porosity content which decreases with the degree of retting, voids being mostly located in the core of samples in a plane parallel to the flow direction. Di Giuseppe et al. (2016) compared X-ray micro-tomography to 2D scanner and an automated fibre analyzer for determining natural fibre length and diameter distributions in PP/miscanthus and PP/hemp biocomposites. The authors concluded that the analysis of lignocellulosic fibers' dimensions in composite materials is complex and that the three techniques used do not allow an unbiased estimation of fibre sizes. Besides, their study highlighted the complementarity of these techniques in terms of length scale.

5.1.2 Nano-mechanical Analysis

Nano-mechanical analysis, which is largely used in polymer tribology,[1] could be useful to characterize the filler/matrix interphase region and evaluate its thickness. Nano-mechanical analysis includes nano-indentation, nano-scratch tests or nano-mechanical imaging techniques, possibly coupled with AFM. All these techniques require the polishing of materials to reduce surface roughness as much as possible.

Nano-indentation tests are able to produce indents of few nanometers in order to measure differences in nano-hardness and Young modulus in the cross-section of composite materials, and thus to highlight the fiber/matrix interphase region. This technique consists in indenting a rigid tip of known geometry, perpendicularly to the material surface and measuring the depth of penetration as a function of the applied load (Downing et al. 2000). Berkvich indenters, i.e. a three-sided triangular-based pyramidal diamond, are commonly used for measurements of mechanical properties at the nanometric scale. This technique has already been applied to wood-reinforced polypropylene composites (Jakes et al. 2007). Authors did not discriminate changes in mechanical properties in the interphase, probably due to the fact that there was no difference. However, they concluded on the need of improving the surface preparation technique. Lee et al. (2007) investigated the hardness and elastic modulus in interphase region of PP/cellulose fibres using

[1]Tribology is the science and engineering of interacting surfaces in relative motion, including the study and application of the principles of friction, lubrication and wear—to characterize the surface properties of polymer films or coatings.

different indentation depths and spacings. The authors showed that nano-indents need to be as small as possible to reduce the zone of analysis and limit the influence of neighbouring material properties.

For nano-scratch tests, the indenter tip is replaced by a scratch tip that scratches the surface in a straight line, crossing matrix and fillers areas. Nano-scratch technique involves moving a sample while it is in contact with a diamond tip. The depth of the indenter is also recorded, thus indicating the hardness of the surface being scratched. The coefficient of friction is determined from the fraction of the lateral and the normal force (this latter being maintained constant). Therefore, the coefficient of friction indicates the resistance of the materials to the tip penetration in the tangential direction. Nano-indentation and nano-scratch techniques can be successfully used if the interface thickness is higher than the penetrating width of the tip, as demonstrated for polymer/glass fibres composites (Hodzic et al. 2000a, b). In the case of nanometric interphases, their thickness can be quantitatively evaluated by mapping the dynamic mechanical property around the interphase region through the use of nano-mechanical imaging techniques. The experimental results show that this method can determine the width and topography of the interphase with nanoscale lateral resolution, as it is for example the case for carbon fibre reinforced polymer composites for which an interface thickness of about 120 nm was evaluated, based on the storage modulus profile on the cross section of the composite (Gu et al. 2010). For the moment, it has only been applied to the characterization of interfaces in polymer micro-composites reinforced with either glass (Kim et al. 2001) or carbon fibres (Gu et al. 2010). Thus, the characterization of polymer/lignocellulosic fibres still remains a challenge.

Finally, abrasion (or scratching) experiments using AFM in contact mode coupled with a simple tribological model could also be a promising way to evaluate differences in nano-mechanical properties between the different phases and at the interface in composite materials (Ahimou et al. 2007, Chichti et al. 2013). This method consists in progressively abrading the surface of the material and simultaneously measuring the shear force. The volume of the material removed by the tip is estimated from the analysis of successive topographic images of the surface, and the shear force is measured by keeping a constant normal force. As previously mentioned, AFM is also a highly useful tool for probing the interphase, because it involves much lower interaction forces between the probe and the sample than nano-indentation (Downing et al. 2000). Thereby, AFM imaging and nano-mechanical measurements are commonly combined (Gao and Mäder 2002; Lee et al. 2007; Young et al. 2013; Cech et al. 2013).

5.2 Mechanical Characterization of the Interphase

5.2.1 Micromechanical Analysis

Among the experimental techniques used for assessing the fibre/matrix interfacial adhesion in composites, micromechanical analyses rely on the study of the

mechanical behaviour of a model microcomposite composed of a single fibre (or a bundle of fibres) embedded in a small volume of the matrix. These analyses allow understanding the interfacial failure mechanisms that occur at the local scale when a fibre undergoes mechanical loads. They are thus relevant to provide quantitative information about the interfacial strength.

Pull-out test is a micromechanical analysis technique that has been widely used for glass fibre reinforced composites and is being adapted to natural fibres. It consists in pulling a fibre out of the matrix which can be a block, a small cylinder or a micro-droplet (case of microbond test) of polymer held by a microvise or blades (Fig. 5.2). The pulling force, which is applied axially by a mechanical testing machine, induces mainly tensile stresses in the fibre and shear stresses at the fibre/matrix interface. The force is monitored while the displacement at the end of the fibre is increased at a constant speed until either pull-out occurs or the fibre breaks. The typical force–displacement curve (Fig. 5.2) exhibits an increase of the force up to a maximum (F_{max}) which corresponds to the total debonding of the fibre, followed by the force drop associated to the release of the adherence and the frictional sliding of the fibre (Miller et al. 1987).

Figure 5.3 shows a typical SEM image of a flax fibre/polyester matrix microbond specimen after debonding. The polyester droplet of 50 µL was deposited on the fibre with a calibrated micro-syringe (Baley et al. 2006).

Based on the measurements of the pull-out force F_{max} and the area A of the embedded length L of fibre within the matrix, the apparent interfacial shear strength τ_{app} (IFSS) is calculated from the Eq. 5.1:

$$\tau_{app} = \frac{F_{max}}{A} \tag{5.1}$$

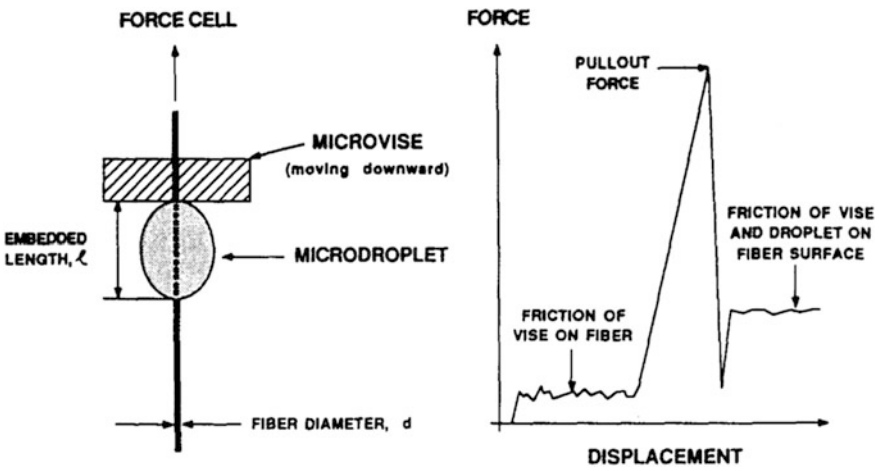

Fig. 5.2 The microbond arrangement (left) and a typical force-displacement record (right). Reprinted from (Miller et al. 1991), Fig. 2. with permission from Elsevier

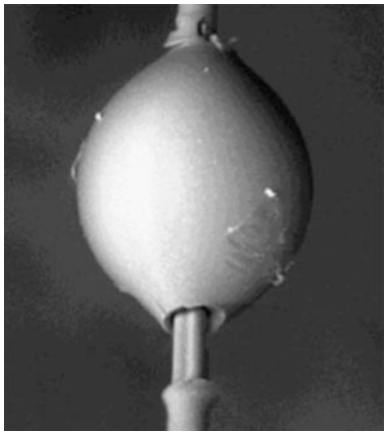

Fig. 5.3 Example of a microdrop of polyester on flax fibre after debonding (fibre diameter: 16 μm). Reprinted from (Baley et al. 2006), Fig. 5. with permission from Elsevier

For a straight fibre with a uniform cross-section, A is the product of the embedded length L by the cross-sectional perimeter. Thus, for a cylindrical fibre with a diameter D, Eq. 5.1 leads to the following expression of the IFSS:

$$\tau_{app} = \frac{F_{max}}{\pi DL} \tag{5.2}$$

Because the cross-section of natural fibres can differ a lot from a regular circular shape (Fig. 5.4), the assessment of the cross-sectional perimeter deduced from the side optical measurement of the fibre can be a major source of error in the IFSS measurement. For IFSS evaluations of flax fibres/unsaturated polyester, (Zhang et al. 2014) demonstrated that the error could reach a factor of three. The authors were able to improve the reliability of the IFSS values thanks to direct measurements of the perimeter from images of the fibre cross-section.

Since the fibre undergoes tensile stress during pull-out, the IFSS measurement requires that the fibre does not break before debonding occurs, thus limiting the embedded length below a specific value. For a cylindrical fibre with a given tensile strength σ, the theoretical limit of the embedded length is given by:

$$L < \frac{D\sigma}{4\tau} \tag{5.3}$$

The definition of apparent interfacial shear strength relies on the assumption that the shear stress distribution is uniform along the embedded length. Several authors proposed advanced models able to account for a realistic stress distribution in the case of regular fibres like glass and carbon fibres (Zhandarov and Mäder 2005; Bergeret and Krawczak 2012). However, their application to fibres with variable shape and roughness along their length like natural fibres is not straightforward. Moreover, studies on natural fibres/polymer matrix systems highlighted the

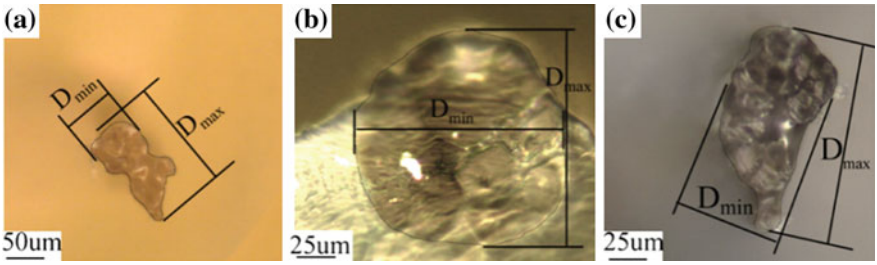

Fig. 5.4 Cross section dimensions of three flax fibres. Reprinted from (Zhang et al. 2014), Fig. 7. with permission from Elsevier

relevance of the post-debonding friction regime in the analysis of the interfacial adhesion (Le Duigou et al. 2013; Yang and Thomason 2010, 2012). It is stated that the corresponding friction strength $\tau_{friction}$ can be related to the residual stresses induced by processing conditions.

A comparison between flax/PLLA and glass/PLLA microbond measurements proposed by (Le Duigou et al. 2012) showed that both systems exhibit similar pull-out force-displacement curves and that the apparent shear strength of the flax/PLLA interface is around twice as high as those of de-sized glass/PLLA (Fig. 5.5 left). It was demonstrated that this discrepancy is the concomitant result of the physico-chemical interactions between the flax surface and PLLA on the one hand and the lower roughness of the de-sized glass fibres (as measured by AFM) on the other hand. In addition, debonding tests performed on single flax fibres treated with release agent in order to weaken the interfacial adhesion confirmed that in that case the only resistance is due to friction (Fig. 5.5 right). This study draws an illustration of the relationship between typical pull-out responses and the behaviour of systems with tailored interfacial adhesion.

The many studies using the pull-out and microbond techniques for natural fibres/polymer matrix systems provide quantitative information relative to the interfacial adhesion and trends about the strategies to enhance it. Thereafter are summarized a few representative examples.

The study of short hemp fibres/PP-MAPP composites highlighted the beneficial effect of a white rot fungi treatment on the IFSS assessed from pull-out measurements (Li et al. 2009). This enzymatic fibre treatment led to an 80% increase of the IFSS, which was clearly visible from the force-displacement curves. It is worth noting that, despite a 28% reduction of the fibres tensile strength and almost no variation of their stiffness, the improvement of the interfacial bonding allowed increasing up to 28% the strength and 62% the stiffness of corresponding tensile composite specimens. The authors correlated the better IFSS to the removal of non-cellulosic compounds (wax, pectin, and lignin) as well as the increased roughness of the fibre surface.

Micromechanical analyses have also been carried out for the interfacial strength of jute and hemp fibres with various polymer matrix composites (Park et al. 2006). The authors proved that the IFSS of the natural fibres/PP significantly increases

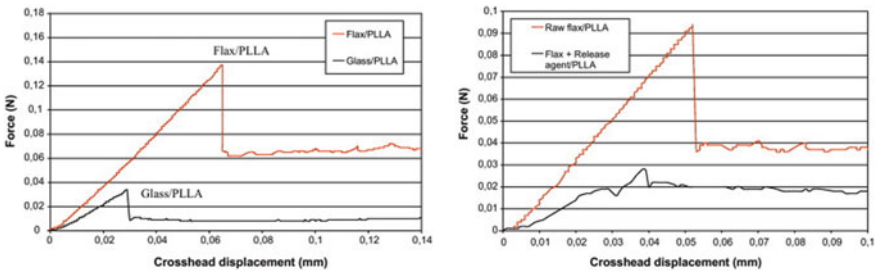

Fig. 5.5 Typical microdroplet test plots for flax/PLLA and de-sized E-glass/PLLA (left); Influence of release agent on microdroplet test for flax/PLLA (right). Reprinted from (Le Duigou et al. 2012) with permission from Elsevier

with increasing the content of MAPP coupling agent within the matrix as well as after treating fibres with alkaline solution and silane coupling agent (Fig. 5.6).

As a comparison, Table 5.1 presents values of the apparent shear stress from debonding tests on single fibre for different natural fibre/polymer matrix systems. Several supplementary results about the IFSS of biocomposites can be found in the literature. For thermoplastic or thermoset matrices associated to different short or long natural fibres: flax (Baley et al. 2006; Le Duigou et al. 2012, 2013; Fuentes et al. 2016), hemp (Li et al. 2009), jute (Park et al. 2008), coir (Tran et al. 2013), bamboo (Fuentes et al. 2015). As discussed in Chap. 4, IFSS is often related to the work of adhesion determined from the surface energies of fibres and matrix. As the interfacial strength can be greatly enhanced by fibre roughness, chemical bonding between the matrix and the fibres, IFSS is not necessarily correlated to the work of adhesion (see Fig. 4.2). Furthermore, Le Duigou et al. (2017) proposed a multiscale analysis of the influence of hygroscopic radial expansion of natural fibres on IFSS in the case of PP/flax biocomposites. They demonstrated that a variation of water content in the composite and thus in flax fibres can be much more influent on the interfacial shear strength than residual stresses induced by the thermomechanical history related to the manufacturing process. Therefore, the processing and design of natural fibre/polymer systems should better take into account their moisture sensitivity that should not only be considered as a drawback, and could play a positive role on interfacial properties if radial stresses are controlled.

Fragmentation test is a technique dedicated to the evaluation of the fibre-matrix adherence inside a composite. It involves the application of increasing axial load to a specimen that contains a single fibre (or bundle or yarn) embedded in the polymer matrix. Load is transferred through the matrix to the fibre by means of the shear stress at the interface. The fibre breakage occurs when this transferred stress reaches locally the tensile strength of the fibre. Kelly and Tyson (1965) reported that when the composite is strained, brittle regular fibres embedded in polymers tend to fracture at the locations of the defects along their length. As the load increases, the fibre continues to fracture into shorter length fragments (Fig. 5.7). The interfacial shear stresses is unable to induce failure stresses in fragments having a length lower

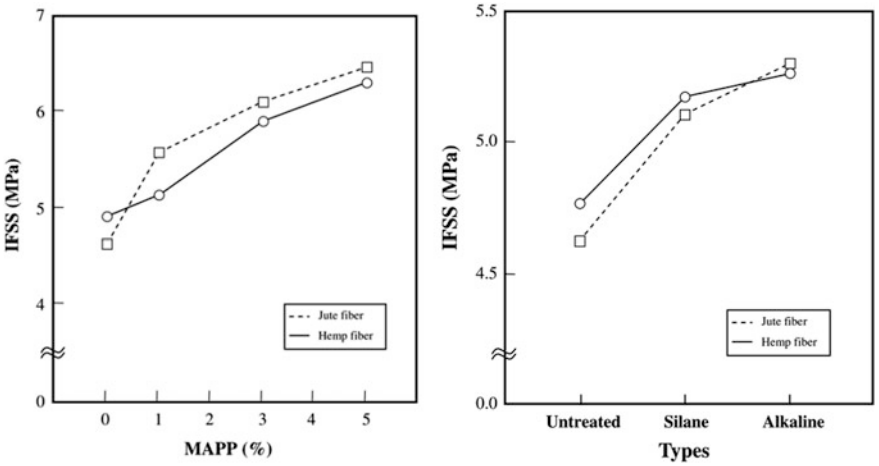

Fig. 5.6 IFSS of jute and hemp fibres/PP with various contents of MAPP coupling agent (left) and fibre treatments (right). Reprinted from (Park et al. 2006) with permission from Elsevier

Table 5.1 Apparent shear stresses (IFSS) determined from debonding tests. Adapted from review tables in (Le Duigou et al. 2012) and (Graupner et al. 2014b)

Fibre type	Matrix	**IFSS** (MPa)	References
Glass	PP	3.3	Le Duigou et al. (2012)
	Epoxy	29.3	
Ananas	PHBV	8.2	Graupner et al. (2014b)
Flax	PLLA (Natureworks)	16.4	Le Duigou et al. (2012)
	PLLA (Biomer)	15.3	
	Epoxy	22.7–23	
	Unsatured polyester	14.2	
	PP	3.4	Graupner et al. (2014b)
	PLA	9–22.2	
	Mater-Bi (Novamont)	4.2	
	PHB	8.8	
Hemp	PP	4.7–9	Le Duigou et al. (2012)
	PP	5.1	Graupner et al. (2014b)
	PLA	11.3	
	Mater-Bi (Novamont)	3	
Henequen	MAPP	4.1	
Jute	PLA	4.6–5.5	
Kenaf	PLA	5.4–10.7	
Lyocell	LDPE	6	
	PP	4.2–5.3	
Ramie	LDPE	10	
	PP	4.9–6	
Sisal	PP	4.6	
	PLA	14.3	
	Mater-Bi (Novamont)	3.2	

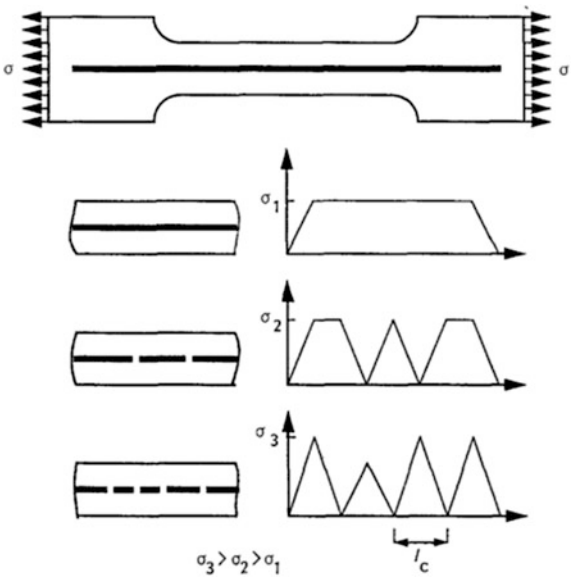

Fig. 5.7 Schematic representation of the single fibre fragmentation test. Reprinted from (Herrera-Franco and Drzal 1992), Fig. 12 with permission from Elsevier

than a specific value L_c, referred as the critical length and considered as an indicator of the interfacial strength. Thus, a decrease of L_c reflects an improvement of the interfacial adhesion and hence the IFSS.

In order to experimentally interpret the failure modes during a fragmentation test, the lengths of the fibre fragments are usually measured using an optical microscope, requiring that the matrix is transparent (Herrera-Franco and Drzal 1992). Theoretically, fragments longer than L_c have been broken into two, yielding a random distribution of fragment lengths between $L_c/2$ and L_c at the end of the fragmentation process. Thereby, the critical length L_c can be deduced from the evaluation of the average $\overline{L}$ of the experimental fragments lengths distribution:

$$L_c = \frac{4}{3}\overline{L} \tag{5.4}$$

Then, according to Kelly and Tyson (1965), the interfacial shear strength τ (IFSS) is calculated from the Eq. 5.5:

$$\tau = \frac{\sigma}{2}\frac{D}{L_c} \tag{5.5}$$

where σ is the fibre tensile strength, D its diameter and L_c the critical length.

To complete the understanding of the complex mechanisms occurring during the fragmentation process, experimental fragmentation testing can be coupled with numerical predictions (Guillebaud-Bonnafous et al. 2012). In that study, a finite element model was developed to simulate the fragmentation process of single hemp

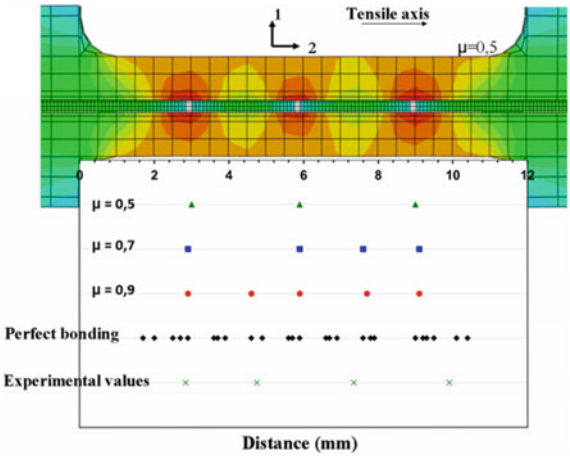

Fig. 5.8 Finite element analysis of the yarn fragmentation locations for different values of the friction coefficient μ and comparison with experimental results. Reprinted from (Guillebaud-Bonnafous et al. 2012) with permission from Elsevier

yarn composite specimens. These simulations, which allowed assessing the sensitivity to the frictional contact coefficient μ (at the fibre/matrix interface), led to results close to the experimental fragmentation patterns and to a comprehensive analysis of the fragmentation test results (Fig. 5.8).

Several studies have provided results about the interfacial properties of natural fibre reinforced thermoplastics. The interfacial shear strength of PE-sisal composites was measured using the single fibre fragmentation test (Torres and Cubillas 2005). Fibre treatment with stearic acid increased the interfacial shear strength by 23% with respect to untreated fibres, which was consistent with SEM observations of failure surfaces. However, the authors discussed the difficulties in obtaining accurate measurements due to the opacity of the matrix and the irregular shape of the natural fibres.

In another study, the interfacial shear strength of a hemp fibre/PP-MAPP composite was evaluated by means of fragmentation testing (Beckermann and Pickering 2009). Based on a mathematical modeling, it was demonstrated that the reinforcing fibres need to be axially aligned in the composite and equal to or longer than 4 L_c in order to achieve the maximum theoretical composite strength.

The mechanical behavior of HDPE reinforced with henequen fibres was studied (Herrera-Franco and Valadez-González 2004). Based on the IFSS measurements of the fragmentation test, the authors showed that fibre-matrix adhesion was improved by the use of a silane coupling agent. It was found that the resulting strength and stiffness of the composite depended on the amount of silane deposited on the fibres. Good correlation was found between the IFSS and the composite tensile strength and an optimal silane concentration was found (Fig. 5.9). From the failure surfaces, it was additionally observed that with increasing fibre-matrix interactions the failure mode changed from adhesive interfacial failure to cohesive interfacial failure occurring in the matrix.

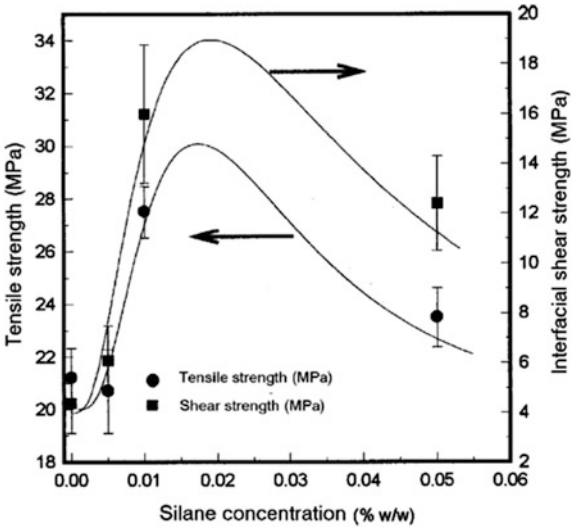

Fig. 5.9 Effect of the concentration of the silane coupling agent solution on the tensile strength and IFSS of henequen–fibre composites. Reprinted from (Herrera-Franco and Valadez-González 2004) with permission from Elsevier

For different thermoplastic matrices (PLA, PP, MAPP) reinforced with Lyocell cellulose fibres, Graupner et al. (2014a) investigated the influence of eucalyptus lignin as a bio-based coupling agent. Lyocell fibres were treated with a lignin-ethanol solution. Fibre/matrix adhesion was assessed using single fibre pull-out and single fibre fragmentation tests. Both testing procedures evidenced the increase of the interfacial shear strength for the lignin-treated fibres (compared with untreated fibres) for all investigated matrices (Fig. 5.10). This improvement was attributed to better chemical interactions between the fibre and matrix and a rougher and larger fibre surface with lignin particles which was revealed by AFM investigations.

In situ tensile test by SEM is a micromechanical characterization technique of composite materials which consists in submitting a coupon to a tensile mechanical loading while observing it by SEM. There have been many studies that deal with the mechanical testing of biocomposites at the macro scale, but very few have reported testing on composites at a micro scale.

The damage mechanisms under stress of flax/PP composite have been studied by in situ SEM observations (Bourmaud et al. 2013). The authors highlighted the influence of the fibre bundles during a tensile experiment. Figure 5.11 shows the occurrence of micro cracks through the transversely oriented fibre bundles, which induce a dislocation between the elementary fibres. This observation evidences that the weakness of natural fibres composites was mainly located at the bundles middle lamellas rather than at the fibre/matrix interface. As a result, the authors postulated that a decrease of the amount of bundles in favour of well dispersed and individualized fibres leads to better mechanical properties of the composite, which can be achieved thanks to an efficient retting of the flax stems.

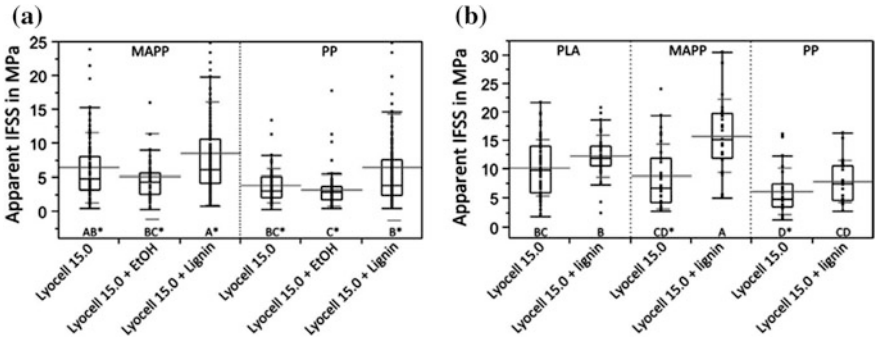

Fig. 5.10 IFSS of untreated, ethanol-treated and ethanol/lignin-treated Lyocell fibres in different matrices measured with the fragmentation (**a**) and pull-out (**b**) tests. Reprinted from Graupner et al. (2014a) with permission from Elsevier

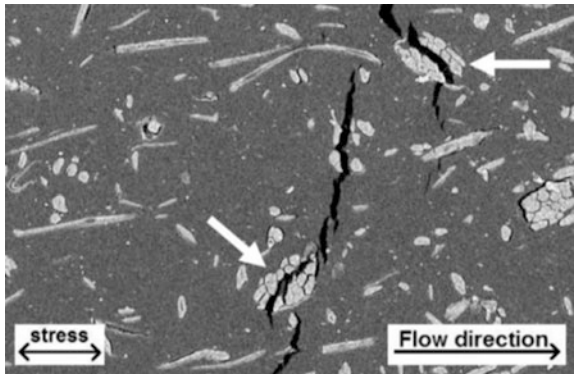

Fig. 5.11 SEM micrograph in the core of PP/flax sample under loading, Reprinted from (Bourmaud et al. 2013) with permission from Elsevier

In a study of the interface in flax/PLA composites modified by organosilane treatments, Le Moigne et al. (2014) conducted SEM observations of crack propagation during tensile test while force-elongation responses were recorded. In order to pick out a region of interest, the coupon was notched on one edge, which induces stress concentrations during the force increments and thus localizes the occurrence of a macrocrack. The SEM observation of the crack tip and margins during its propagation gave access to the analysis of the fibres behaviour under stress within the matrix (Fig. 5.12). Due to the notched, the breakage of the samples occurs by tearing and is not brittle. This experiment could be assimilated to a pull-out test at a larger scale, i.e. several fibres are progressively extracted from the matrix during the crack propagation. Results expressed clearly that the alkaline/GPS silane-treated biocomposites showed a cohesive interfacial failure at much higher loads, as confirmed by the force-elongation curves (Fig. 5.13), which brings out the higher

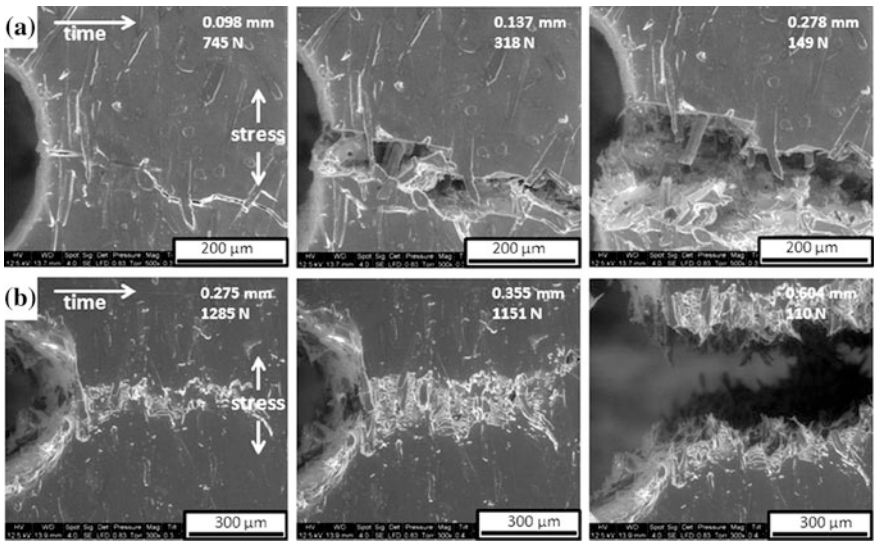

Fig. 5.12 SEM observations during crack propagation in notched specimens for PLA/20% flax **a** non-treated **b** alkaline/GPS silane-treated. Reprinted from Le Moigne et al. (2014) with permission from Elsevier

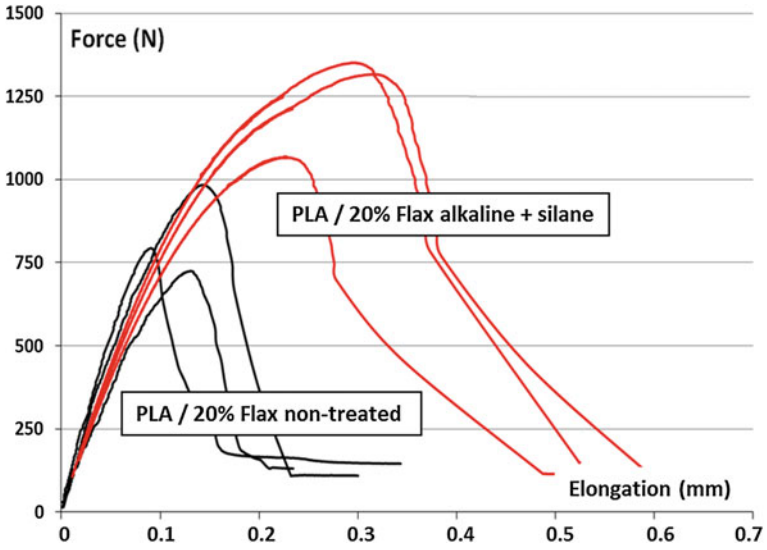

Fig. 5.13 Tensile force-elongation curves recorded during in situ tensile test by SEM for PLA/20% flax non-treated and alkaline/silane-treated (three tests per biocomposites). Reprinted from Le Moigne et al. (2014) with permission from Elsevier

load transfer from the PLA to the treated flax fibres, and hence the greater interfacial adhesion.

5.2.2 *Static Mechanical Analysis*

Static mechanical testing of coupons at the macroscopic scale is the most common technique used for assessing the mechanical performances of composite materials. The shape and dimensions of the coupons are usually imposed by the loading conditions and the eventual corresponding standards. However, the sensitivity of the static mechanical properties to the interfacial adhesion is highly variable between the different possible loading conditions, the nature of the induced stresses and the microstructure of the composite.

In a review of the properties of unidirectional fibre composites, Agarwal et al. (2006) established a qualitative summary of the typical influence of fibres, matrix and interface on the properties of these composites. The results, which are compiled in Table 5.2, are applicable provided that the Young's modulus of the fibres is at least ten times higher than that of the matrix. This summary highlights that the mechanical properties which prove to be actually sensitive to the interfacial adhesion are the tensile transverse strength, the in-plane shear strength and the interlaminar shear strength (Fig. 5.14). The influence of the interface on the other mechanical properties is found to be weak or negligible. Thus, the choice of mechanical tests that are likely to evidence these interface-influenced properties should be prefered in order to assess the interfacial adhesion in unidirectional polymer composites.

As mentioned by Marrot et al. (2014) in a study of the interfacial adhesion between flax fibres and biobased thermoset matrices, several macroscopic

Table 5.2 Summary of the typical influence of constituents on properties of unidirectional polymer composites. S = strong influence, W = weak influence, N = negligible influence. Adapted from (Agarwal et al. 2006)

Composite property	Fibres	Matrix	Interface
Tensile properties			
Longitudinal modulus	S	W	N
Longitudinal strength	S	W	N
Transverse modulus	W	S	N
Transverse strength	W	S	**S**
Compression properties			
Longitudinal modulus	S	W	N
Longitudinal strength	S	S	N
Transverse modulus	W	S	N
Transverse strength	W	S	N
Shear properties			
In-plane shear modulus	W	S	N
In-plane shear strength	W	S	**S**
Interlaminar shear strength	N	S	**S**

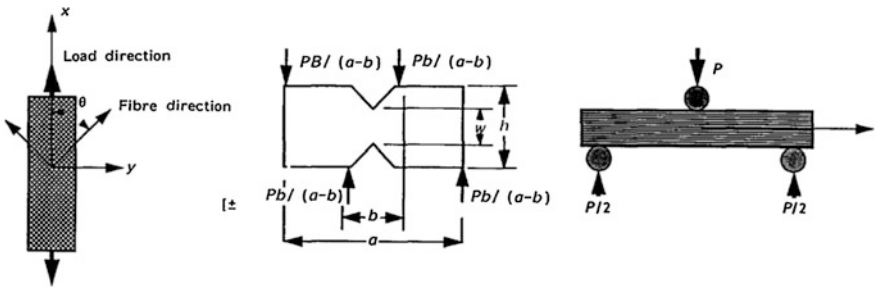

Fig. 5.14 Schematic representation of several shear tests: ±45 tension, Iosipescu and short beam shear (from left to right), Reprinted from (Herrera-Franco and Drzal 1992) with permission from Elsevier

mechanical tests are sensitive to the interfacial properties: transverse tensile, in-plane ±45 tension, Iosipescu and short-beam shear tests (Fig. 5.14), which are still not widely used for biocomposites. In that study, the interlaminar shear strength (ILSS) was assessed using in-plane tension shear test on ±45 flax laminates manufactured with the different petrochemical and biobased matrices, and the ILSS results were compared to IFSS measurements determined via the debonding test. A strong positive correlation between the ILSS and the IFSS was highlighted (Fig. 5.15). In parallel, tensile mechanical properties of unidirectional (UD) flax fibres composites based on the same matrices were measured. As expected, the Young's modulus of the UD composites was primarily determined by the fibres and matrices stiffness and the fibre volume fraction according to the mixing rule, showing virtually no relationship with the interlaminar shear strength.

Among the possible methods that allow evaluating the ILSS of composites, the **short-beam shear test** is performed with a three-points bending specimen (Fig. 5.14) with a low span-to-thickness ratio, typically in the range 4 to 5, in order to induce interlaminar failure due to shear stresses. The interlaminar shear strength τ of the specimen is calculated from the Eq. 5.6:

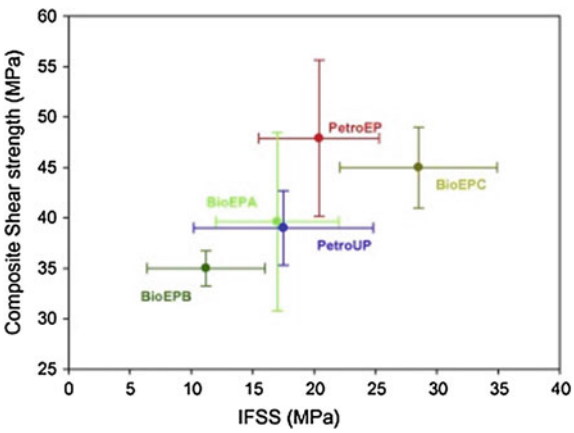

Fig. 5.15 Shear strength (ILSS) of the ±45 laminates versus microscopic IFSS given by the microbond test. Reprinted from Marrot et al. (2014) with permission from Elsevier

$$\tau = \frac{3}{4}\frac{F_{max}}{A} \tag{5.6}$$

where F_{max} is the load at failure and A the transverse cross-sectional area.

The main advantage of the short-beam test is its simplicity comparatively to other current ILSS test methods, which involve complex setups or special sample machining.

In a study about jute/polyester composites, Sever et al. (2012) proposed several fabrics surface treatments in order to enhance the interfacial adhesion. Jute fabrics were modified by alkali, micro-emulsion silicon and fluorocarbon based agents. ILSS were evaluated by short-beam shear tests and IFSS from pull-out tests. All surface treatments improved both the IFSS and ILSS of the composites, the maximum improvement being obtained with the fluorocarbon based agents. Tensile measurements evidenced that the proposed treatments improved the modulus and strength of the composites, accordingly.

Acoustic emission (AE) is a non-destructive method based on the statistical analysis of the elastic waves produced by the different failures in a coupon during a tensile test and measured at its surface by high sensitivity piezoelectric (PZT) sensors. AE allows monitoring the types of fracture sources and their progress during the test by analyzing parameters such as energy, amplitude, and frequency emitted from fibre failures, matrix cracking, and fibres debonding. Moreover, the combination of several PZT sensors enables the localization of the different events inside the coupon. Acoustic emission real-time monitoring has been successfully used on traditional polymer composites reinforced with carbon or glass fibres. However, experimental difficulties may arise in the case of natural fibres composites, mainly because of the scattering in fibres properties and the less pronounced acoustic emission activity than in traditional composites.

As reviewed by Romhány et al. (2003) and De Rosa et al. (2009) and other authors, acoustic emission was used to monitor the failure modes in flax bundles during a single fibre fracture test, showing that an AE range of amplitudes can be assigned to the main failure mechanisms (Fig. 5.16). The authors also showed that AE can be used to identify the failure mode sequence of flax fibre reinforced thermoplastic composites during a tensile test, and that the AE amplitudes of the different failure events follows the subsequent ranking: (i) fibre/matrix debonding, as well as the axial split of the pectin boundary layer between the elementary flax fibres (ii) fibre pull-out, as well as formation of microcracks within the elementary flax fibres (iii) fibre breakage.

Assarar et al. (2011) used the acoustic emission technique to study the influence of water ageing on tensile mechanical properties and damage events in flax–fibre/epoxy composites (compared with glass–fibre/epoxy composites). In this study, the AE signals analysis was based on several parameters: the amplitude, the energy, the duration, the rise time and the events counts. These collected parameters were used as input descriptors in a specific classification method which allows identifying each damage mechanisms and to follow their progress until the final global failure of the tensile sample. For the aged flax composite samples, it was shown that the AE activities start from the beginning of the tensile test (Fig. 5.17), which was not

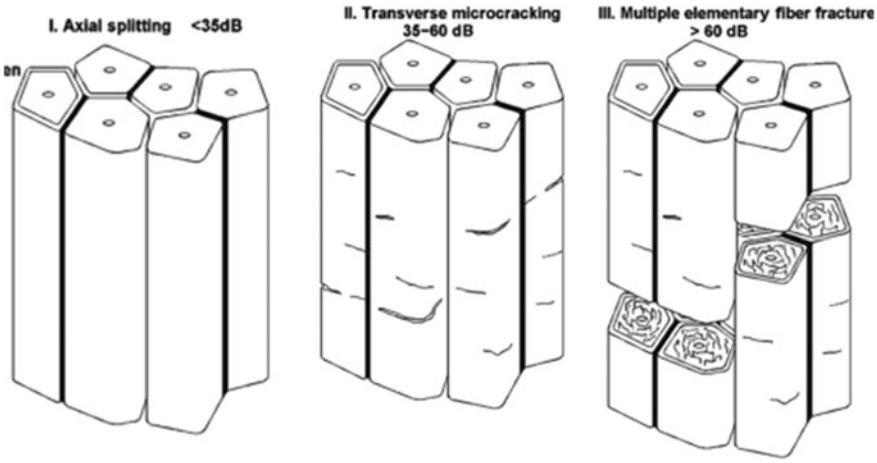

Fig. 5.16 Schematic lay-up of the failure sequence along flax bundle with the related AE amplitude ranges (from left to right): (I) axial splitting of elementary fibres (AE amplitude <35 dB), (II) transverse microcracking of elementary fibres (AE amplitude 35–60 dB), (III) multiple fracture of flax bundle (AE amplitude >60 dB). Adapted from De Rosa et al. (2009) with permission from Elsevier

noticed for unaged samples or for the glass–fibres reinforced composite. Combined with the absence of fibre-matrix debonding signals after ageing, this led the authors to the conclusion that fibre/matrix interface weakening was the main damage mechanism induced by water ageing for flax composites.

5.2.3 *Dynamic Mechanical Analysis*

Dynamic mechanical analysis (DMA) also called **dynamic mechanical thermal analysis** (DMTA), is a technique dedicated to the assessment of the viscoelastic behaviour of materials, mainly polymers and composites. A specimen is submitted to sinusoidal stress in tension, bending, shearing or torsion and the resulting strain is measured, allowing determining the stress/strain ratio as a complex modulus. The temperature of the specimen or the loading frequency is swept in order to investigate the resulting variations of the complex modulus. The real part *E'* of the complex modulus, known as the *storage modulus*, is a measure of the elastic character of the material, while the imaginary part *E"*, known as the *loss modulus*, is a measure of its viscous character. The ratio of the loss and storage moduli, defined as the *damping factor* (or loss factor) $\tan\delta = E''/E'$, is related to internal frictions and is sensitive to different kinds of molecular motions, relaxation processes, thermal transitions and structural heterogeneities. A typical DMA graph of the evolution of storage modulus, loss modulus and $\tan\delta$ versus temperature is shown in Fig. 5.18. The maximum values of the damping factor are located at

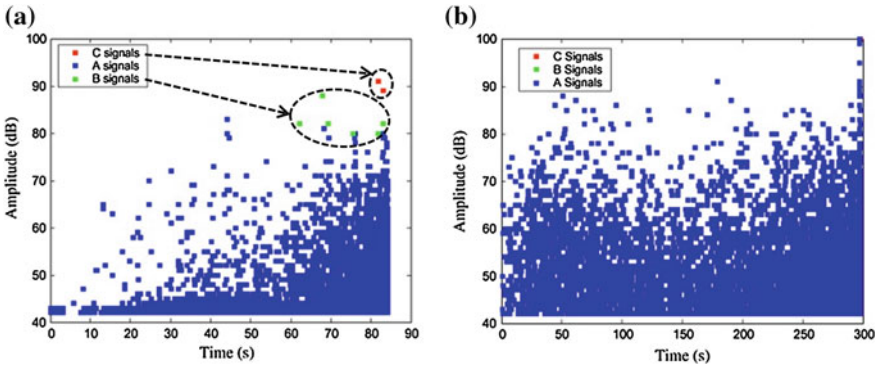

Fig. 5.17 AE signals versus tensile tests time for flax–fibre reinforced composites, unaged (**a**) and after 20 days of immersion into a water bath at room temperature (**e**). A signals: matrix cracking, B signals: fibre–matrix debonding and C signals: fibre failure. Adapted from Assarar et al. (2011) with permission from Elsevier

specific temperatures associated to polymer chains relaxations such as the glass transition *Tg*. In the vinicity of the *Tg*, the α transition is usually characterized by a prominent peak, being more pronounced with increasing amorphous polymer fraction. Other transitions associated to smaller molecular motions are visible at lower temperatures, i.e. β and γ transitions.

Energy dissipation in composites, which is expressed by the damping factor measured by DMA, depends on the intrinsic viscoelastic properties of the individual components, their volume fractions and arrangement in the composite and also the interfacial adhesion between the fibre and the matrix. A poorly bonded interface potentially leads to local sliding-friction mechanisms and thus to additional global dissipation which tends to increase the damping factor while a strong interface cohesion tends to decrease it. Thus, the variations of the damping factor can be used as an indication of the interfacial adhesion in composites.

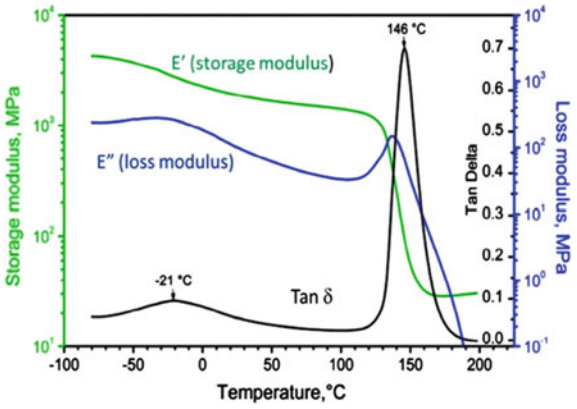

Fig. 5.18 Typical DMA graph of the evolution of storage modulus, loss modulus and tan δ versus temperature. Reprinted from Saba et al. (2016), with permission from Elsevier

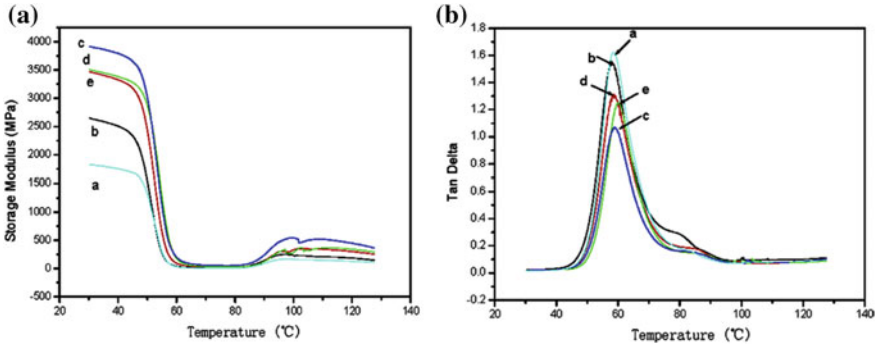

Fig. 5.19 Temperature dependence of storage modulus (A) and damping factor (B) of PLA and PLA-based composites: neat PLA (a), composite with untreated fibres (b), composite with alkali treated fibres (c), composite with APS silane treated fibres (d), composite with GPS silane treated fibres (e). Reprinted from Yu et al. (2010), Fig. 5 with permission from Elsevier

In a study about PLA/ramie composites, Yu et al. (2010) conducted dynamic mechanical analyses which highlight the effect of fibre surface treatments on the viscoelastic properties of the composites. Figure 5.19 displays the comparison of the temperature dependence of the storage modulus and the damping factor for neat PLA and PLA-based composites (with untreated fibres and with fibres treated by alkali and silanes). The increase of the storage modulus at ambient temperature with the presence of the ramie fibres confirms their reinforcement capability which is additionally improved by the tested fibre treatments, especially the alkali one. The storage modulus of all samples drops at around 60 °C. The damping factor exhibits a maximum for this temperature, which can be associated to the glass transition temperature of the system. The amplitude of the damping peak of the treated composites decreases in comparison to neat PLA and untreated composites, which indicates that the treatments decreased the molecular mobility of macromolecular chains at the fibre/matrix interface due to an improved compatibility between PLA matrix and ramie fibres. The strength of the same materials, which was measured by flexural tests, resulted in the same ranking, confirming the efficiency of the alkali and silane treatments to enhance interfacial adhesion and hence the composites' performances.

Many other studies about natural fibre reinforced polymeric matrix composites confirmed that the presence of fibres tends to directly influence the intensity of the damping factor in the vicinity of the main relaxation transition of the polymer matrix (Abdelmouleh et al. 2007; Idicula et al. 2005; Le Moigne et al. 2014; Mohanty et al. 2006; Pothan et al. 2003; Romanzini et al. 2013). A reason of the intensity reduction, is that there is less matrix by volume to dissipate the vibration energy, assuming that the damping factor of the matrix is higher than that of the fibres at the considered temperature. Moreover, fibres and favourable fibre/matrix interactions can reduce the mobility of polymer chains, leading to lower degrees of molecular motion and hence lower damping factors.

A possible quantification of the dissipation associated to the interface relies to the definition of an interfacial damping factor $\tan \delta_{in}$ calculated from the difference between the actual measured damping factor $\tan \delta$ of a composite and the theoretical damping factor $\tan \delta_c$ of the corresponding fibre-matrix system:

$$\tan \delta_{in} = \tan \delta - \tan \delta_c \tag{5.7}$$

There exist several models for estimating the theoretical damping factor $\tan \delta_c$ of the composite (Dong and Gauvin 1993). A simple model relies on the rule of mixture applied to the intrinsic damping ratios of the components:

$$\tan \delta_c = V_f \tan \delta_f + \left(1 - V_f\right) \tan \delta_m \tag{5.8}$$

where V_f, $V_m\left(= 1 - V_f\right)$ and $\tan \delta_f$, $\tan \delta_m$ are the volume fraction and the damping ratio of the fibre and the matrix, respectively.

When the damping factor of the matrix becomes much higher than the damping factor of the fibre, which usually occurs for a polymer in the vicinity of its main relaxation temperature, Eq. 5.8 simplifies in:

$$\tan \delta_c = \left(1 - V_f\right) \tan \delta_m \tag{5.9}$$

In order to account for the variable level of the interactions between polymer and fibres, Ziegel and Romanov (1973) proposed an interfacial adhesion factor B and a rewriting of Eq. 5.9 as follows:

$$\tan \delta_c = \left(1 - BV_f\right) \tan \delta_m \tag{5.10}$$

B is a correction parameter that can be related to the effective thickness of the fibre/matrix interphase around the fibres. The stronger the interfacial interactions, the thicker the immobilized layer of polymer chains and the higher the value of parameter B (Dong and Gauvin 1993).

In a study about the interface in flax/PLA composites, Le Moigne et al. (2014) evaluated the influence of organosilane treatments on the viscoelastic behavior of the biocomposites submitted to a temperature ramp. The authors focused their discussion on the damping factor measurements in the vicinity of the main relaxation temperature. Incorporating non-treated flax fibres in the matrix led to a strong decrease of the damping, which was amplified by the treatments. The authors completed their analysis of the interface by calculating from Eq. 5.10 the value of parameter B for the different biocomposites. Based on the results of parameter B and considering an elementary fibre of 20 μm in diameter, it was possible to calculate an equivalent thickness of interphase (Fig. 5.20). The resulting values of interphase thickness were in agreement with those reported in literature for other composites systems based on glass fibres. The corresponding improvements of the interfacial adhesion were also consistent with the increased stiffness and strength measured for the treated biocomposites.

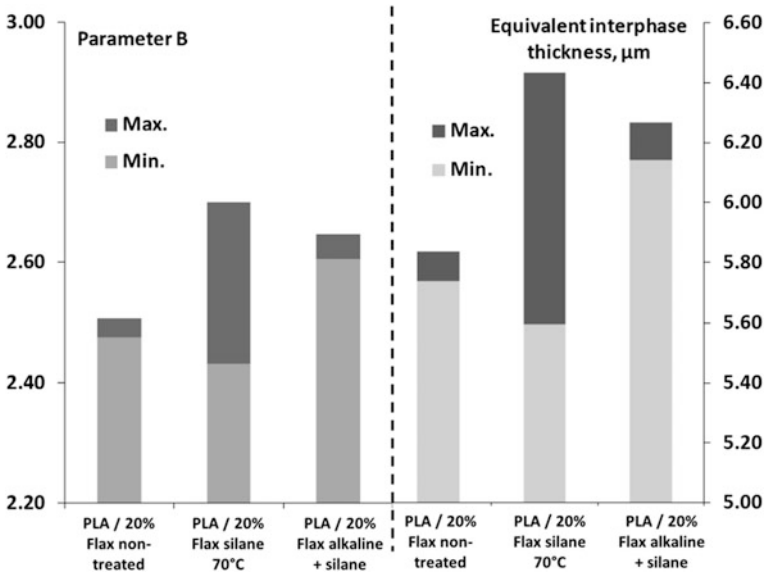

Fig. 5.20 Values of parameter B from Eq. (5.10) and equivalent interphase thickness for the different PLA/flax biocomposites. Reprinted from Le Moigne et al. (2014), with permission from Elsevier

5.3 Thermal Analysis of the Interphase

Thermal analysis is defined by the IUPAC (International Union of Pure and Applied Chemistry) recommendations (Lever et al. 2014) and ICTA (International Confederation for Thermal Analysis) publications (Lombardi 1980) as including all techniques in which a sample property is measured versus temperature. It includes thermogravimetry analysis (TGA) and differential scanning calorimetry (DSC) that will be detailed below, but also dielectric thermal analysis (DEA), dynamic mechanical analysis (DMA detailed in the previous section), thermoluminescence (TL), thermomechanical analysis (TMA), thermodilatometry (TD) and so on.

Thermogravimetry analysis (TGA) is commonly used to determine selected characteristics of materials that exhibit mass loss due to decomposition, oxidation, or loss of volatiles such as moisture. Differential scanning calorimetry (DSC) measures differences in heat flow inputs into a sample and a reference when they are subjected to a controlled temperature program. Practically, all physical and chemical processes involve changes in enthalpy or specific heat. For example, as a solid sample melts, higher heat flow will be required to maintain the sample temperature at the temperature of the reference. Melting is thus an endothermic phase transition. Likewise, as the sample undergoes exothermic processes, such as crystallization, less heat is required to maintain sample temperature at the reference temperature. These phase transitions are first-order transitions. The glass transition characterized by a sudden increase of molecular mobility manifests itself in DSC by a second-order transition, i.e. an endothermic jump in the heating curve.

5.3.1 Thermogravimetry Analysis

The thermal stability of untreated natural fibres has been widely studied. A three-step process is commonly suggested. The first mass-loss occurring between 25 and 150 °C is generally associated to dehydration of chemically bound moisture (up to 10%). Hemicelluloses decomposition may also occur in this range up to 180 °C. Lignin begins to decompose at 160 °C and continues up to 400 °C. Cellulose decomposition is the third step that occurs between 200 and 300 °C with a rapid mass loss between 300 and 360 °C. As already exposed in Chap. 4 Sect. 4.5.1, the presence of grafted molecules onto natural fibres modifies their thermal stability. In the case of alkaline and acetylated treatments, hemicellulose and lignin extraction induces an improvement of the thermal stability of natural fibres in the temperature range 250–350 °C. Moreover TGA curves exhibited higher temperature peaks for alkali pre-treated acetylated fibres (Kabir et al. 2013). As concerns natural fibres treated by enzymes, George et al. (2014) concluded that enzymes can be used to address the limited thermal stability of natural fibres by selectively removing the least thermally stable pectic and hemicellulosic components. Physical treatments such as plasma treatments did not really influence the thermal stability of natural fibres as shown by Sinha (2009) and more recently by Scalici et al. (2016). Finally the effects of silane treatments were also investigated by Kabir et al. (2013). No change was observed as concerned hemicellulose decomposition in comparison to untreated fibres, indicating that silane treatments did not remove hemicellulose and that silane grafting protected the fibre from thermal decomposition at higher temperatures. In the case of alkali pre-treated silanised fibres, an enhancement of the thermal resistance at 250–300 °C was observed.

Only few papers studied the effect of natural fibres surface treatments on the thermal stability of biocomposites themselves. Pracella et al. (2010) showed a lower thermal stability of PP/hemp fibres biocomposites when a maleic anhydride modified PP is introduced or when maleic anhydride grafted hemp fibres are used. On the contrary, Sisti et al. (2016) give evidence of a greater thermal stability of PBS biocomposites containing retted hemp fibres compared to PBS/unretted hemp biocomposites, in agreement with TGA results carried on fibres alone. But major papers are generally focused on the development of specific flame retardants grafted onto natural fibres (Shumao et al. 2010; Chen et al. 2011; Suardana et al. 2011; Dorez et al. 2014a). Dorez et al. (2014a) showed a loss of thermal stability of polybutylene succinate (PBS)/flax fibres biocomposites when fibres are grafted with different phosphorus compounds. Phosphorylation of flax fibres that occurs at low temperatures seemed to favour their dehydration inducing both an enhancement of the residue formation and PBS degradation. An increase of the residue with the grafting rate was observed and the action was stronger with phosphorus-based molecules (such as dihydrogen ammonium phosphate DAP) compared to phosphonated polymers (poly-dimethyl(methacryloxy)methyl phosphonate homopolymer or corresponding copolymer with methylmethacrylate). It was assumed that only a part of phosphonic acid functions of each polymer chain was covalently

bonded onto the fibre surface contrary to DAP. Moreover the advantage provided by the grafting strategy of phosphonated molecules onto the natural fibres and their localization at the interface was pointed out compared to additive strategy of the same molecules in PBS (Dorez et al. 2014b). Recently Fan and Naughton (2016) suggested a mechanism describing the decomposition steps close to the fibre/matrix interface in the case of hemp fibre reinforced polyester composites. These authors observed that an increase in temperature leads successively (i) to primary cell wall decomposition and interfacial separation due to fibre shrinkage, (ii) then to secondary cell wall decomposition (which are lignin poor) within the char region, and (iii) finally to lignin rich primary cell walls decomposition leading to a deeply blackened but still intact region. When ignition occurred, fibres are completely decomposed leaving a residue of charred material and voids (Fig. 5.21).

Concluding, TGA is considered to highlight the improvement of the thermal stability of natural fibres after surface modification. But up to only few studies were focused on the understanding of the thermal degradation mechanisms within biocomposites in relation to the fibre/matrix interface and its modification.

5.3.2 Differential Scanning Calorimetry

Differential scanning calorimetry (DSC) can be used to study the effect of fibres surface treatments on the crystallization of polymer matrices. Surface and resulting interface modifications can influence two main factors as regard to the polymer crystallization in composites: (i) the nucleating effect of fibres that influences the crystallization kinetics, and (ii) the steric hindrance induced by fibre/matrix interactions that alters the growth of the polymeric crystals and could inhibit crystallization.

Generally, an increase in the crystallinity ratio is obtained and is associated to the appearance of a transcrystalline region at the fibre/matrix interface. This increase can reach up to 9% as shown by Joseph et al. (2003) studying the influence of hemp fibres surface modifications (isocyanate-based treatment, oxidative treatment by KMnO4) and by Pracella et al. (2010) analysing the effect of the addition of maleic anhydride modified PP, both in the case of PP/hemp biocomposites. Similar tendencies were also observed for poly(hydroxybutyrate-co-valerate) (PHBV) reinforced by torrefied wheat straw fibres (Berthet et al. 2016) and for poly (lactic acid) (PLA) reinforced by acetylated cellulose fibres (Spiridon et al. 2016). Wang et al. (2011) found that alkali or aminosilanes (APS) had little or no influence on the nucleation ability of sisal fibres in sisal/PLA biocomposites. In contrast, Sisti et al. (2016) give evidence of a decreased PBS crystallinity when retted hemp fibres are used compared to unretted ones, probably due to propounced steric hindrance thanks to stronger chemical interactions between the matrix and the fibres. Similar conclusions were proposed by Le Moigne et al. (2014) for silanised or alkali pre-treated silanised flax fibres incorporated in PLA and by Bourmaud and Baley (2007) with addition of maleic anhydride grafted PP in PP/hemp biocomposites. The authors attributed the decreased nucleating effect of the treated fibres to enhanced interactions between the matrix and the fibres that immobilize polymer chains at the fibres surface.

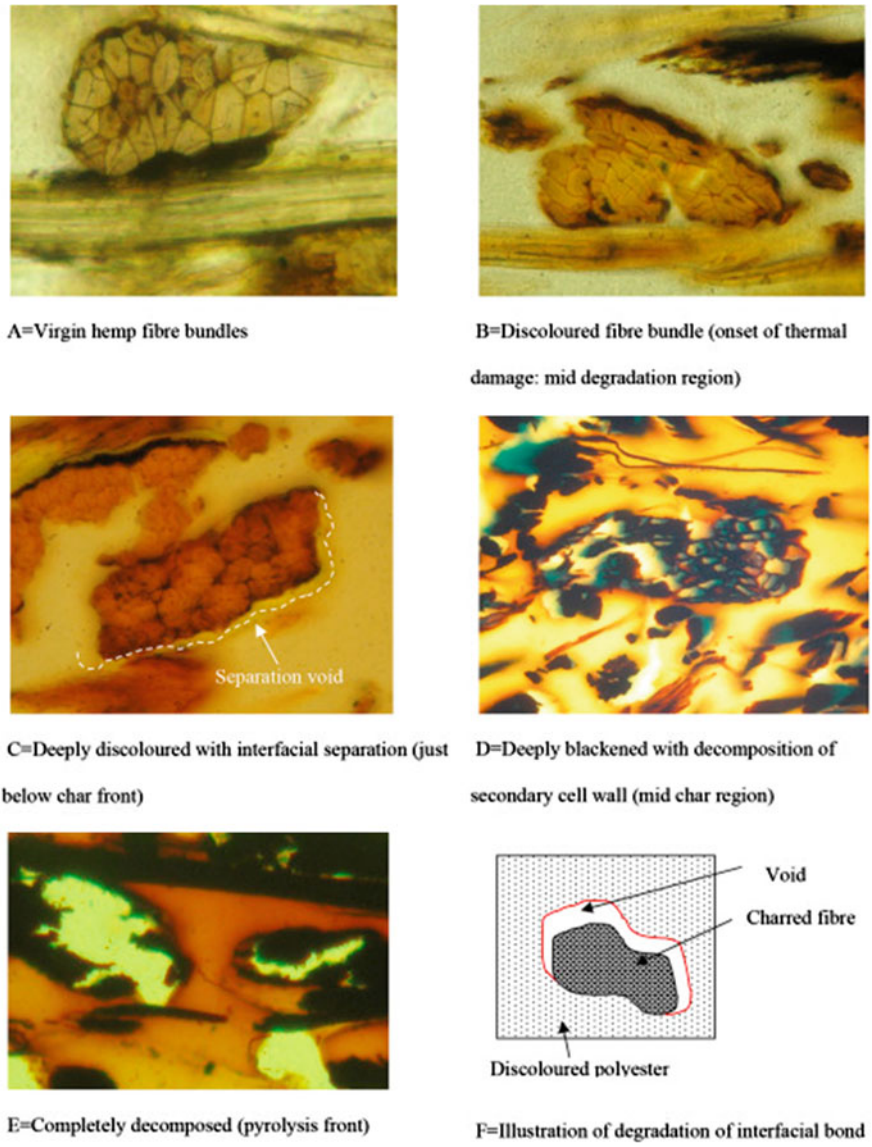

Fig. 5.21 (from A to E) Progressive steps of the decomposition of a hemp fibres reinforced polyester biocomposite located at the fibre/matrix interface; (F) Illustration of degradation of interfacial bond. Reproduced from Fan and Naughton (2013) with permission from Elsevier

Furthermore, variations in the glass transition temperature *Tg* related to changes in molecular mobility in the interphase zone can also be detected. As an example, Le Moigne et al. (2014) measured a positive shift of the glass transition temperature *Tg* of about 2 °C in silane treated flax fibres/PLA composites which was attributed

to reduced molecular mobility of PLA chains in the interphase zone due to enhanced fibre/matrix interactions. In this regard, Lipatov (1977) and later Théocaris (1987) proposed relations allowing to evaluate the interphase thickness in filled polymer systems based on the measurement of the variation of thermal capacity of the composite at the glass transition temperature *Tg*. For fibre reinforced composites, Eq. 5.11 was proposed:

$$\left(\frac{\Delta r_i + r_f}{r_f}\right)^2 - 1 = \frac{\lambda v_f}{1 - v_f} \tag{5.11}$$

with r_f the radius of the fibres, Δri the interphase thickness, vf the fibre volume fraction, λ an interaction parameter related to the fraction of macromolecular chains whose mobility is reduced in the interphase zone and $\lambda = 1 - \Delta C_p^c / \Delta C_p^m$, with ΔC_p^c the variation of thermal capacity of the composite at *Tg*, and ΔC_p^m the variation of thermal capacity of the matrix at *Tg*. Correlation between the interphase thickness evaluated by Eq. 5.11 and the tensile strength of sized glass fibre composites/PP has been found (Karian 1996). Nevertheless, this model has not been applied yet to natural fibre reinforced composites.

Concluding, changes in the polymer crystallization and glass transition in bio-composites related to surface treatments and fibre/matrix interactions are considered as relevant phenomena when studying the interfacial properties in natural fibre based composites. Opposite trends are observed depending on the nature of surface modifications of natural fibres. New developments on high performing microscopic techniques, such as atomic force microscopy AFM, coupled with thermal analysis should allow to progress in the understanding of macromolecular organization and interactions at the interphase in natural fibre reinforced composites.

5.4 Concluding Remarks

Although numerous studies investigated the development of natural fibres treatments intended to improve the interfacial adhesion with polymer matrices, no standardized methods for quantifying the quality of the interphase within natural fibre reinforced composites emerge, and various approaches are currently developed. They benefit from the recent development of new means of observation and characterization techniques as Atomic Force Microscopy (AFM) or X-ray computed tomography which make it possible to study the interphase region at the nanometric scale. It should be pointed out that the study of the interphase in such material cannot be based on a single "universal" technique and generally requires a set of experimental techniques and eventually modelling approaches which each provides information on the interphase. When evaluating the efficiency of a specific natural fibre treatment and its effect on the interfacial properties of a composite material, a multi-technique approach should thus be conducted:

- **Microscopic observations** (optical, SEM, X-ray tomography…) would provide (i) qualitative information on the microstructure of the matrix/reinforcement interphase zone (cohesion, trancrystallinity) and the interfacial breakage mechanisms (failure surface by SEM), and (ii) quantitative informations can be obtained by image analysing with measurements of microstructural parameters such as distribution and orientation of reinforcements, or (iii) local mechanical measurements in the interphase region (AFM, nano-indentation…);
- **Physico-chemical characterizations** of natural fibres and their composites are likely to provide information in terms of (i) chemistry: elemental composition, chemical structure of the functionalizing molecules and nature of the chemical bonds with matrix or the fibres (AES, ToF-SIMS, XPS, EDX, NMR, IR, Raman, GPC…), (ii) physico-chemistry and topography: surface energy, polarity (contact angle, IGC) and roughness (AFM) of the fibres (iii) physics: crystallisation and relaxation phenomena related to the mobility of macromolecular chains of the polymer matrix and/or coupling agent in the interphase zone (DSC);
- **Micromechanical analyzes** (pull-out, fragmentation, in situ tensile test by SEM) allow to assess (i) the mechanical behaviour and failure mechanisms at the interface and (ii) the interfacial shear strength (IFSS) between the reinforcement and the matrix for a single fibre model composite, being far from a real composite material;
- **Dynamic mechanical analysis** (DMA/DMTA) gives specific information on (i) the viscoelastic behaviour of the composites and (ii) relaxation phenomena related to the mobility of macromolecular chains of the polymer matrix and/or coupling agent in the interphase zone and can be coupled with DSC analysis;
- **Static mechanical analysis** (tensile, shear) would provide information on (i) the macroscopic mechanical behaviour of the composites at small strain (stiffness, visco-elasticity), (ii) their mechanisms of damage at large strain (ductility, ultimate strength, ILSS), thus indirectly characterizing the consequences of the quality of the interfacial adhesion.

References

Abdelmouleh M, Boufi S, Belgacem M, Dufresne A (2007) Short natural–fibre reinforced polyethylene and natural rubber composites: Effect of silane coupling agents and fibres loading. Compos Sci Technol 67:1627–1639

Ahimou F, Semmens MJ, Novak P, Haugstad G (2007) Biofilm cohesive measurement using a novel atomic force microscopy methodology. Appl Environ Microbiol 73(9):2897–2904

Alemdar A, Zhang H, Sain M, Cescutti G, Müssig J (2008) Determination of fiber size distributions of injection moulded polypropylene/natural fibers using x-ray microtomography. Adv Eng Mater 10:126–130

Assarar M, Scida D, El Mahi A, Poilâne C, Ayad R (2011) Influence of water ageing on mechanical properties and damage events of two reinforced composite materials: flax–fibres and glass–fibres. Mater Des 32:788–795

Agarwal BD, Broutman LJ, Chandrashekhara K (2006) Analysis and performance of fiber composites. Wiley

Baley C, Busnel F, Grohens Y, Sire O (2006) Influence of chemical treatments on surface properties and adhesion of flax fibre–polyester resin. Compos Part A Appl Sci Manuf 37:1626–1637
Beckermann GW, Pickering KL (2009) Engineering and evaluation of hemp fibre reinforced polypropylene composites: micro–mechanics and strength prediction modelling. Compos Part A Appl Sci Manuf 40:210–217
Bergeret A, Krawczak P (2012) Liaison renfort/ matrice– Définition et caractérisation. Techniques de l'Ingénieur 33:1–25
Berthet MA, Angellier-Coussy H, Machado D, Hilliou L, Staebler A, Vicente A, Gontard N (2015) Exploring the potentialities of using lignocellulosic fibres derived from three food by–products as constituents of biocomposites for food packaging. Ind Crops Prod 69:110–122
Berthet MA, Commander JM, Rouau X, Gontard N, Angellier Coussy H (2016) Torrefaction treatment of lignocellulosic fibres for improving fibre/matrix adhesion in a biocomposite. Mater Des 952:223–232
Bledzki AK, Jaszkiewicz A (2010) Mechanical performance of biocomposites based on PLA and PHBV reinforced with natural fibres—A comparative study to PP. Compos Sci Technol 70 (12):1687–1696
Bourmaud A, Baley C (2007) Investigations on the recycling of hemp and sisal fibre reinforced polypropylene composites. Polym Degrad Stab 92:1034–1045
Bourmaud A, Ausias G, Lebrun G, Tachon ML, Baley C (2013) Observation of the structure of a composite polypropylene/flax and damage mechanisms under stress. Ind Crops Prod 43:225–236
Cech V, Palesch E, Lukes J (2013) The glass Fiber–polymer matrix Interface/interphase characterized by nanoscale imaging techniques. Compos Sci Technol 83:22–26
Chen D, Li J, Ren J (2011) Combustion properties and transference behaviour of ultrafine microencapsulated ammonium polyphosphate in ramie fabric–reinforecd poly(L–lactic acid) biocomposites. Polym Int 60(4):599–606
Chichti E, George M, Delenne JY, Radjai F, Lullien-Pellerin V (2013) Nano–mechanical properties of starch and gluten biopolymers from atomic force microscopy. Eur Polym J 49 (12):3788–3795
De Rosa IM, Santulli C, Sarasini F (2009) Acoustic emission for monitoring the mechanical behaviour of natural fibre composites: a literature review. Compos Part A Appl Sci Manuf 40:1456–1469
Di Giuseppe E, Castellani R, Dobosz S, Malvestio J, Berzin F, Beaugrand J, Delisée C, Vergnes B, Budtova T (2016) Reliability evaluation of automated analysis, 2D scanner, and micro-tomography methods for measuring fiber dimensions in polymer-lignocellulosic fiber composites. Compos Part A Appl Sci Manuf 90:320–329
Dong S, Gauvin R (1993) Application of dynamic mechanical analysis for the study of the interfacial region in carbon fiber/epoxy composite materials. Polym Compos 14:414–420
Dorez G, Otazaghine B, Taguet A, Ferry L, Lopez Cuesta JM (2014a) Improvement of the fire behaver of poly(1,4–butanediol succinate)/flax biocomposites by fiber surface modification with hosphorus compounds: molecular versus macromolecuar strategy. Polym Int 63(9):1665–1673
Dorez G, Taguet A, Ferry L, Lopez Cuesta JM (2014b) Phosphorous compounds as flame retardants for polybutylene succinate/flax biocomposites: Additive versus reactive route. Polym Degrad Stab 102:152–159
Downing TD, Kumar R, Cross WM, Kjerengtroen L, Kellar JJ (2000) Determining the interphase thickness and properties in polymer matrix composites using phase imaging atomic force microscopy and nanoindentation. J Adhes Sci Technol 14(14):1801–1812
Effah B, Van Reenen A, Meincken M (2015) Characterization of the interfacial adhesion of the different components in wood–plastic composites with AFM. Springer Sci Reviews 3:97–111
Fan M, Naughton A (2016) Mechanisms of thermal decomposition of natural fibre composites. Compos B 88:1–10
Fuentes CA, Brughmans G, Tran LQN, Dupont-Gillain C, Verpoest I, Van Vuure AW (2015) Mechanical behaviour and practical adhesion at a bamboo composite interface: physical adhesion and mechanical interlocking. Compos Sci Technol 109:40–47
Fuentes CA, Ting KW, Dupont-Gillain C, Steensma M, Talma AG, Zuijderduin R, Van Vuure AW (2016) Effect of humidity during manufacturing on the interfacial strength of non–pre–dried flax fibre/unsaturated polyester composites. Compos Part A Appl Sci Manuf 84:209–215

Gao SL, Mäder E (2002) Characterization of interphase nanoscale property variations in glass fiber reinforced poypropylene and epoxy resin composites. Compos Part A Appl S 33:559–576
George J, Sreekala MS, Thomas S (2001) A review on interface modification and characterization of natural fiber reinforced plastic composites. Polym Eng Sci 41:1471–1485
George M, Mussone PG, Bressler DC (2014) Surface and thermal characterization of natural fibres treated with enzymes. Ind Crops Prod 53:365–373
Graupner N, Fischer H, Ziegmann G, Müssig J (2014a) Improvement and analysis of fi–bre/matrix adhesion of regenerated cellulose fibre reinforced PP–, MAPP– and PLA–composites by the use of Eucalyptus globulus lignin. Compos Part B Eng 66:117–125
Graupner N, Rößler J, Ziegmann G, Müssig J (2014b) Fibre/matrix adhesion of cellulose fibres in PLA, PP and MAPP: A critical review of pull–out test, microbond test and single fibre fragmentation test results. Compos Part A Appl Sci Manuf 63:133–148
Gu Y, Li M, Wang J, Zhang Z (2010) Characterization of the interphase in carbon fiber/polymer composites using a nanoscale dynamic mechanical imaging technique. Carbon 48(11):3229–3235
Guillebaud-Bonnafous C, Vasconcellos D, Touchard F, Chocinski-Arnault L (2012) Experimental and numerical investigation of the interface between epoxy matrix and hemp yarn. Compos Part A Appl Sci Manuf 43:2046–2058
Herrera-Franco PJ, Drzal LT (1992) Comparison of methods for the measurement of fibre/matrix adhesion in composites. Composites 23:2–27
Herrera-Franco P, Valadez-González A (2004) Mechanical properties of continuous natural fibre–reinforced polymer composites. Compos Part A Appl Sci Manuf 35:339–345
Hodzic A, Stachurski ZH, Kim JK (2000a) Nano–indentation of polymer–glass interfaces. Part I. Experimental and mechanical analysis. Polymer 41:6895–6905
Hodzic A, Kim JK, Stachurski ZH (2000b) The nano–scratch technique as a novel method for measurement of an interphase width. J Mater Sci Lett 19:1665–1667
Idicula M, Malhotra SK, Joseph K, Thomas S (2005) Dynamic mechanical analysis of randomly oriented intimately mixed short banana/sisal hybrid fibre reinforced polyester composites. Compos Sci Technol 65:1077–1087
Jakes JE, Hermanson JC, Stone DS (2007) Nanoindentation of the interphase region of a wood–reinforced polypropylene composite. In: 9th International conference on wood & biofiber plastic compsites. Wisconsin (USA)
Joseph PV, Joseph K, Thomas S, Pillai CKS, Prasad VS, Groeninckx G, Sarkissova M (2003) The thermal and crystallisation studies of short sisal fibre reinforced polypropylene composites. Compos Part A Appl Sci Manuf 34:253–266
Kabir MM, Wang H, Lau KT, Cardona F (2013) Effects of chemical treatment on hemp fibre structure. Appl Surf Sci 276:13–23
Karian HG (1996) Designing interphases for mega-coupled polypropylene composites. Plast Eng 52(1):33–35
Kastner J, Plank B, Reh A, Salaberger D, Heinzl C (2012) Advanced x–ray tomographic methods for quantitative characterisation of carbon fibre reinforced polymers. In: 4th International symposium on NDT in aerospace. We.3.A.1
Kelly A, Tyson WR (1965) Tensile properties of fibre–reinforced metals: copper/tungsten and copper/molybdenum. J Mech Phys Solids 13:329–350
Kim JK, Sham ML, Wu J (2001) Nanoscale characterisation of interphase in silane treated glass fibre composites. Compos Part A Appl S 32:607–618
Le Duigou A, Bourmaud A, Balnois E, Davies P, Baley C (2012) Improving the interfacial properties between flax fibres and PLLA by a water fibre treatment and drying cycle. Ind Crops Prod 39:31–39
Le Duigou A, Davies P, Baley C (2013) Exploring durability of interfaces in flax fibre/epoxy micro–composites. Compos Part A Appl Sci Manuf 48:121–128
Le Duigou A, Merotte J, Bourmaud A, Davies P, Belhouli K, Baley C (2017) Hygroscopic expansion: A key point to describe natural fibre/polymer matrix interface bond strength. Compos Sci Technol 151:228–233

Le Moigne N, Longerey M, Taulemesse JM, Bénézet JC, Bergeret A (2014) Study of the interface in natural fibres reinforced poly(lactic acid) biocomposites modified by optimized organosilane treatments. Ind Crops Prod 52:481–494

Lee SH, Wang S, Lee S-H (2007) Evaluation of interphase properties in a cellulose fiber–reinforced polypropylene composite by nanoindentation and finite element analysis. Compos Part A Appl S 38(6):1517–1524

Lever T, Haines P, Rouquerol J, Charsley EL, Van Eckeren P, Burlett DJ (2014) ICTAC nomenclature of thermal analysis (IUPAC Recommandations 2014). Pure Appl Chem 86(4):545–553

Li Y, Pickering KL, Farrell RL (2009) Determination of interfacial shear strength of white rot fungi treated hemp fibre reinforced polypropylene. Compos Sci Technol 69:1165–1171

Lipatov YS (1977) Physical chemistry of filled polymers. In: Moseley RJ (ed) International polymer science and technology monograph, vol 2, Moscou

Théocaris PS (1987) The mesophase concept in composites. Springer, Verlag Berlin

Lombardi G (1980) For better thermal analysis, 2nd edn. ICTA, Rome

Ludueña L, Vázquez A, Alvarez V (2012) Effect of lignocellulosic filler type and content on the behavior of polycaprolactone based eco–composites for packaging applications. Carbohydr Polym 87:411–421

Mai K, Mäder E, Mühle M (1998) Interphase characterization in composites with new non–destructive methods. Compos Part A Appl S 29:1111–1119

Marrot L, Bourmaud A, Bono P, Baley C (2014) Multi–scale study of the adhesion between flax fibers and biobased thermoset matrices. Mater Des 62:47–56

Martin N, Mouret N, Davies P, Baley C (2013) Influence of the degree of retting of flax fibers on the tensile properties of single fibers and short fiber/polypropylene composites. Ind Crops Prod 49:755–767

Miller B, Muri P, Rebenfeld L (1987) A microbond method for determination of the shear strength of a fiber/ resin interface. Compos Sci Technol 28:17–32

Miller B, Gaur U, Hirt DE (1991) Measurement and mechanical aspects of the microbond pull–out technique for obtaining fiber/resin interfacial shear strength. Compos Sci Technol 42:207–219

Mohanty S, Verma SK, Nayak SK (2006) Dynamic mechanical and thermal properties of MAPE treated jute/HDPE composites. Compos Sci Technol 66:538–547

Nikishkov Y, Airoldi L, Makeev A (2013) Measurement of voids in composites by X–ray Computed Tomography. Compos Sci Technol 89:89–97

Park JM, Quang ST, Hwang BS, De Vries KL (2006) Interfacial evaluation of modified Jute and Hemp fibers/polypropylene (PP)–maleic anhydride polypropylene copolymers (PP–MAPP) composites using micromechanical technique and nondestructive acoustic emission. Compos Sci Technol 66:2686–2699

Park JM, Kim PG, Jang JH, Wang Z, Hwang BS, DeVries KL (2008) Interfacial evaluation and durability of modified Jute fibers/polypropylene (PP) composites using micromechanical test and acoustic emission. Compos Part B Eng 39:1042–1061

Pothan LA, Oommen Z, Thomas S (2003) Dynamic mechanical analysis of banana fiber rein–forced polyester composites. Compos Sci Technol 63:283–293

Pracella M, Haque MMU, Alvarez V (2010) Functionalization, compatibilization and properties of polyolefin composites with natural fibers. Polymers 2:554–574

Rials TG, Wolcott MP, Nassar JM (2001) Interfacial contributions in lignocellulosic fiber–reinforced polyurethane composites. J Appl Polym Sci 80(4):546–555

Romanzini D, Lavoratti A, Ornaghi HL, Amico SC, Zattera AJ (2013) Influence of fiber content on the mechanical and dynamic mechanical properties of glass/ramie polymer composites. Mater Des 47:9–15

Romhány G, Karger-Kocsis J, Czigány T (2003) Tensile fracture and failure behavior of thermoplastic starch with unidirectional and cross–ply flax fiber reinforcements. Macromol Mater Eng 288:699–707

Saba N, Jawaid M, Alothman OY, Paridah MTT (2016) A review on dynamic mechanical properties of natural fibre reinforced polymer composites. Constr Build Mater 106:149–159

Scalici T, Fiore V, Valenza A (2016) Effect of plasma treatment on the properties of Arundo Donax L. leaf fibres and its bio–based epoxy composies; A preliminary study. Composites Part B Eng 94:167–175
Sever K, Sarikanat M, Seki Y, Erkan G, Erdoğan ÜH, Erden S (2012) Surface treatments of jute fabric: the influence of surface characteristics on jute fabrics and mechanical properties of jute/polyester composites. Ind Crops Prod 35:22–30
Shumao L, Jie R, Hua Y, Tao Y, Weizhong Y (2010) Influence of ammonium polyphosphate on the flame retardancy and mechanical properties of ramie fiber–reinforced poly(lactic acid) biocomposites. Polym Int 59(2):242–248
Singh AP, Anderson R, Park BD, Nuryawan A (2013) A novel approach for FE–SEM imaging of wood–matrix polymer interface in a biocomposite. Micron 54–55:87–90
Sinha E (2009) Effect of cold plasma treatment on macromolecular structure, thermal and mechanical behaviour of jute fiber. J Ind Text 38(4):317–339
Sisti L, Totaro G, Vannini M, Fabbri P, Kalia S, Zatta A, Celli A (2016) Evaluation of retting process as a pre–treatment of vegetable fibers for the preparation of high–performance polymer biocomposites. Ind Crops Prod 81:56–65
Spiridon I, Darie RN, Kangas H (2016) Inlfuence of fiber modifications on PLA/fiber composites. Behavior to accelerated weathering. Composites Part B Eng 92:19–27
Suardana NPG, Ku MS, Lim JK (2011) Effects of diammonium phosphate on the flammability and mechanical properties of biocomposites. Mater Des 32:1990–1999
Tillman MS, Hayes BS, Seferis JC (2000) Analysis of polymeric composite interphase regions with thermal atomic force microscopy. J Appl Polym Sci 80:1643–1649
Torres FG, Cubillas ML (2005) Study of the interfacial properties of natural fibre reinforced polyethylene. Polym Test 24:694–698
Tran LQN, Fuentes CA, Dupont-Gillain C, Van Vuure AW, Verpoest I (2013) Understanding the interfacial compatibility and adhesion of natural coir fibre thermoplastic composites. Compos Sci Technol 80:23–30
Wang Y, Tong B, Hou S, Li M, Shen C (2011) Transcrystallization behavior at the poly(lactic acid)/sisal fibre biocomposite interface. Compos Part A Appl S 42:66–74
Wright JR, Mathias LJ (1993) Physical characterization of wood and wood–polymer composites: an update. J Appl Polym Sci 48(12):2225–2239
Wurm A, Ismail M, Kretzschmar B, Pospiech D, Schick C (2010) Retarded crystallization in polyamide/layered silicates nanocomposites caused by an immobilized interphase. Macromolecules 43:1480–1487
Yang L, Thomason JL (2010) Interface strength in glass fibre–polypropylene measured using the fibre pull–out and microbond methods. Compos Part A Appl S 41:1077–1083
Yang L, Thomason JL (2012) Development and application of micromechanical techniques for characterising interfacial shear strength in fibre–thermoplastic composites. Polym Test 31:895–903
Yang P, Elhajjar R (2014) Porosity content evaluation in carbon fibre/epoxy composites using X–ray computed tomography. Polymer-Plastics Technol Eng 53:217–222
Young TJ, Crocker LE, Broughton WR (2013) Observations on interphase characterisation in polymer composites by nano–scale indentation using AFM and FEA. Compos Part A Appl S 50:39–43
Yu T, Ren J, Li S, Yuan H, Li Y (2010) Effect of fiber surface–treatments on the properties of poly (lactic acid)/ramie composites. Compos Part A Appl Sci Manuf 41:499–505
Zhandarov S, Mäder E (2005) Characterization of fiber/matrix interface strength: applicability of different tests, approaches and parameters. Compos Sci Technol 65:149–160
Zhang D, Milanovic NR, Zhang Y, Su F, Miao M (2014) Effects of humidity conditions at fabrication on the interfacial shear strength of flax/unsaturated polyester composites. Compos Part B Eng 60:186–192
Ziegel KD, Romanov A (1973) Modulus reinforcement in elastomer composites. II polymeric fillers. J Appl Polym Sci 17:1133–1142